



GHGT-12

## Capturing the coupled hydro-mechanical processes occurring during CO<sub>2</sub> injection – example from In Salah

Tore Ingvald Bjørnarå<sup>a,b,c,\*</sup>, Simon A. Mathias<sup>a</sup>, Jan M. Nordbotten<sup>b</sup>, Joonsang Park<sup>c</sup>,  
Bahman Bohloli<sup>c</sup>

<sup>a</sup>Durham University, Dept. Earth Sciences, Durham, UK

<sup>b</sup>University of Bergen, Dept. of Mathematics, Bergen, Norway

<sup>c</sup>NGI, Dept. of Petroleum Geomechanics and Geophysics, Oslo, Norway

---

### Abstract

At In Salah, CO<sub>2</sub> is removed from the production stream of several natural gas fields and re-injected into a deep and relatively thin saline formation, in three different locations. The observed deformation on the surface above the injection sites have partly been contributed to expansion and compaction of the storage aquifer, but analysis of field data and measurements from monitoring has verified that substantial activation of fractures and faults occur. History-matching observed data in numerical models involve several model iterations at a high computation cost. To address this, a simplified model that captures the key hydro-mechanical effects, while retaining a reasonable accuracy when applied to realistic field data from In Salah, has been derived and compared to a fully resolved model. Results from the case study presented here show a significant saving in computational cost (36%) and a computational speed-up factor of 2.7.

© 2014 The Authors. Published by Elsevier Ltd. This is an open access article under the CC BY-NC-ND license (<http://creativecommons.org/licenses/by-nc-nd/3.0/>).

Peer-review under responsibility of the Organizing Committee of GHGT-12

*Keywords:* CO<sub>2</sub> storage; In Salah; two-phase flow; poroelasticity; vertical equilibrium; linear vertical deflection

---

---

\* Corresponding author. Tel.: +47 22023000; fax: +47 22230448.  
E-mail address: [tore.ingvald.bjornara@ngi.no](mailto:tore.ingvald.bjornara@ngi.no)

## Nomenclature

$b$	Biot's coefficient, $b = 1 - K/K_s$ , [-]
$\beta, \gamma$	fitting parameters in capillary pressure function: $p_d = \beta + \gamma$ , [Pa]
$c_\alpha$	compressibility of fluid phase $\alpha$ , [1/Pa]
$\varepsilon_v$	volumetric strain, [-]
$\mathbf{f}$	volumetric body load vector, [N/m <sup>3</sup> ]
$\phi$	porosity, [-]
$\mathbf{g}$	gravity vector, [m/s <sup>2</sup> ]
$\mathbf{I}$	identity matrix, [-]
$\mathbf{k}$	permeability, [m <sup>2</sup> ]
$k_{r\alpha}$	relative permeability of phase $\alpha$ , [-]. Here: $k_{rn} = s_n^p$ and $k_{rw} = (1-s_n)^q$
$K$	bulk modulus of (drained) porous media, [Pa]
$K_s$	bulk modulus of solid grain, [Pa]
$\mu_\alpha$	viscosity of phase $\alpha$ , [Pa·s]
$p_\alpha$	pressure of phase $\alpha$ , [Pa]
$p_p$	pore pressure, [Pa]
$p_c$	capillary pressure, phase pressure difference; $p_c = p_n - p_w$ , [Pa]
$p_d$	entry pressure, pressure required for non-wetting phase to intrude wetting phase, [Pa]
$p, q$	fitting parameters (exponent) for the power-law relative permeability functions $k_{r\alpha}$ , [-]
$\mathbf{q}_\alpha$	Darcy flux of phase $\alpha$ , [m/s]
$\rho_\alpha$	density of phase $\alpha$ , [kg/m <sup>3</sup> ]
$s_\alpha$	saturation of phase $\alpha$ , [-]
$\boldsymbol{\sigma}$	total stress tensor, [Pa]
$\boldsymbol{\sigma}'$	effective stress, [Pa]
$t$	time, [s]
$\mathbf{v}_\alpha$	velocity of fluid phase $\alpha$ , [m/s]
$\mathbf{v}_s$	velocity of solid phase, [m/s]

## 1. Introduction

At In Salah, CO<sub>2</sub> is removed from the production stream of several natural gas fields and re-injected into a deep and relatively thin saline formation, approximately 20 meters thick, at about 1800 meters below surface. CO<sub>2</sub> is injected into three locations; wells KB-501, -502 and -503, and the injection has been actively monitored. Of particular interest are the InSAR-surveys, that monitors the surface deformation, and tracers in the injected CO<sub>2</sub>, that allows detection of the injected CO<sub>2</sub> in monitoring wells. The InSAR-data has revealed a surface heave rate of up to 5 mm/year on all the three injection wells, and a corresponding subsidence at the gas-producing wells of about 2 mm/year [11].

Due to the relatively poor hydraulic properties of the aquifer, 1-1.5 km long horizontal injection wells are used to ensure adequate injection rates and approximately 0.6 Mton CO<sub>2</sub> is sequestered per year all together [5]. The surface heave/subsidence is caused primarily due to expansion/compaction of the aquifer/reservoir caused by the CO<sub>2</sub> injection/gas production [8]. However, at injection well KB-502 there are two distinctive lobes in the heave pattern at the surface that have caught a lot of attention as to how this can be explained. It was suggested early that this was due to a long structural discontinuity; a non-sealing fault/fracture system, that is activated by tensile strains [13,15,17] due to its orientation in line with the direction of the maximum horizontal stress (a strike-slip stress regime [6,8]). Tracers in the injected CO<sub>2</sub> at KB-502 also showed up in a monitoring well (KB-5) about three times faster than what would have occurred with an homogeneous cylindrical plume [14], again, indicating a highly permeable pathway in line with the strike-slip stress regime. And, indeed such a fault/fracture system (labelled F12) was later confirmed by updated seismic surveys and further supported by numerical modeling studies [13,15,17]. F12 cuts through the aquifer, but how far it extends in the vertical direction is not well constrained. Modeling has suggested that it may be confined within the aquifer [13] or that it may extend into the lowermost part of the overburden [9,15].

In all the injection wells the formation bottom hole pressure (FBHP) may exceed the fracture pressure of the aquifer [3]. Analysis of the injectivity index (volumetric injection rate of CO<sub>2</sub> versus FBHP) indicates that fractures are activated/deactivated during injection, depending on increasing/decreasing injection rate, respectively, and this is particularly the case for KB-501 and -502 [3]. Several authors, eg. [3,13,17], have history-matched the bottom hole pressure with numerical models and have obtained very good fits with measured surface heave. However, as observed from the injectivity index analysis, for wells KB-501 and -502 it is necessary to mimic the activation of fractures by introducing a transient permeability, to the aquifer, and transmissibility of the fault system F12. This dynamic behavior is consistent with stress analysis (related to fracture pressure) and field observations [17]. Also, the subsurface at In Salah has a layered structure, but how many distinctive layers that is used in the literature varies, along with the hydraulic and mechanical properties of the aquifer, F12, caprock and over- and underburden.

This variation in model realizations encountered in the literature shows that there are many possible explanations to the observed measurements. However, it often requires many model iterations to find a good fit between modelled and measured data, which can be computationally very expensive and time consuming. To address this, we have in this study applied the assumption that the thickness of the storage aquifer is much smaller than both the lateral extent of the aquifer and the length-scale of interest, to derive a simplified model that captures the key hydro-mechanical effects. The goal is to derive a computationally efficient, yet accurate, model that can be used in analysis where large numbers of simulations are required. The simplified model is compared with a fully resolved synthetic CO<sub>2</sub> injection model, based on conditions in In Salah, to see how well it performs in terms of accuracy and computational cost and time.

## 2. Modeling approaches

The geomechanical effects related to CO<sub>2</sub> injection at In Salah are analyzed through fully coupled modeling approaches to simulate simultaneously CO<sub>2</sub> migration in the aquifer and the poroelastic stress changes during injection.

In the first approach, a fully resolved model where the complete geometry is discretized and the governing equations for two-phase immiscible fluid flow in porous media (with capillary pressure) and poroelasticity (using Biot's linear theory of poroelasticity) are solved using the finite element method. The critical area, in terms of numerical resolution, is the aquifer where the CO<sub>2</sub> is injected and a dense numerical discretization is required to capture its migration and distribution to a sufficient accuracy.

In the second approach, a simplified description of the physical processes in the aquifer is derived using the method of reduction of dimensionality. It involves integrating the governing equations over the thickness of the aquifer, transforming relevant variables and equations into integrated and averaged quantities and equations that are only functions of spatial variables on a plane. This reduces the computational cost by reducing the number of degrees of freedom (DOF) needed to be solved.

For two-phase flow, reduction of dimensionality involves integrating the fluid mass conservation equations to obtain the Vertical Equilibrium (VE) equations, see eg. Nordbotten and Dahle [10]. The assumption for VE is that the vertical flow can be ignored (is zero), implying that the vertical pressure gradient is static (in vertical equilibrium) and proportional to the specific gravity of the pore fluid. For the poroelasticity, it involves integrating the momentum balance equation to obtain the poroelastic Linear Vertical Deflection (PLVD) equation. The assumptions for PLVD is that (i) the vertical momentum is zero, (ii) the in-plane displacement components are constant across the thickness of the aquifer and (iii) the out-of-plane displacement component varies linearly. The PLVD equation is similar to the ones obtained by Bear and Corapcioglu [1], however, here we treat the aquifer as an embedded region in a fully three dimensional environment, accounting for the full stress tensor in the over- and underlying layers, and extend the pore fluid to also include two phases [4].

In this study, the performance of the two approaches are compared, and the applicability of the simplified model is demonstrated on realistic field data from In Salah. Wells KB-501 and -503 behaves more predictable compared to KB-502, as they do not show a similar critical feature like fault 12 at KB-502. However, KB-501 also show fracture activation [3], so the focus will be on well KB-503.

### 3. Governing equations

The physics related to CO<sub>2</sub> injection into subsurface can be described by the momentum balance equation under quasi-static conditions (neglecting inertial terms) and the mass conservation equations of two-phase fluid (brine and CO<sub>2</sub>) which are given in the following form:

$$\nabla \cdot \boldsymbol{\sigma} + \mathbf{f} = 0 \quad (1)$$

$$\frac{\partial(\phi \rho_\alpha s_\alpha)}{\partial t} + \nabla \cdot (\phi \rho_\alpha s_\alpha \mathbf{v}_\alpha) = 0 \quad (2)$$

The Darcy flux vector  $\mathbf{q}_\alpha$  in a deforming medium is defined as:

$$\mathbf{q}_\alpha = s_\alpha \phi (\mathbf{v}_\alpha - \mathbf{v}_s) = -\frac{\mathbf{k}}{\mu_\alpha} k_{r\alpha} (\nabla p_\alpha - \rho_\alpha \mathbf{g}) \quad (3)$$

The effective stress  $\boldsymbol{\sigma}'$  is defined as the part of the total stress  $\boldsymbol{\sigma}$  that governs the deformation, and using the concept of Terzaghi effective stress, Biot [2] modified the normal elastic stress terms in the momentum balance equation so the total stress term in Eq. (1) can be written as:

$$\boldsymbol{\sigma} = \boldsymbol{\sigma}' + b p_p \mathbf{I} \quad (4)$$

By inserting Eq. (3) into Eq. (2) and rearranging (following the procedure of Pinder [12], considering the relations for change in porosity and change in volumetric strain [18, chapter 1 and 4] and using the mass conservation equation for the solid phase) a familiar equation can be obtained for the mass conservation equation for phase  $\alpha$ :

$$\phi \rho_\alpha \frac{\partial s_\alpha}{\partial t} + \phi s_\alpha \rho_\alpha c_\alpha \frac{\partial p_\alpha}{\partial t} + s_\alpha \rho_\alpha \left[ \frac{(b - \phi)}{K_s} \frac{\partial p_p}{\partial t} - b \frac{\partial \varepsilon_v}{\partial t} \right] + \nabla \cdot (\rho_\alpha \mathbf{q}_\alpha) = 0 \quad (5)$$

It can be seen that Eq. (5) is the same flow equation obtained by Biot [2] for a single-phase fluid by inserting that  $s_\alpha = 1$  and using that, in the context of multiphase flow, the pore pressure  $p_p$  in Eqs. (4) and (5) is defined as the saturation-weighted average of the phase pressure;  $p_p = s_w p_w + s_n p_n$ .

In Eq. (5) there are four dependent variables;  $s_w$ ,  $p_w$ ,  $s_n$  and  $p_n$ , but only two conservation equations, so two of the variables can be eliminated by applying the constraint for a fully saturated rock:  $s_w + s_n = 1$ , and by introducing the capillary pressure  $p_c$  defined as the difference between the phase pressures;  $p_c = p_n - p_w$ . Here  $p_c$  is a Brooks and Corey-type function of the non-wetting saturation  $s_n$ :

$$p_c(s_n) = \beta (1 - s_n)^{-1/2} + \gamma \quad (6)$$

Eqs. (1) and (5) are the governing equations that are solved with appropriate boundary conditions described in the next section. Since the aquifer is considered essentially horizontal, the equivalent governing equations for the dimensionally reduced model, using the VE and PLVD assumptions, are the same equations integrated in the vertical direction from the bottom to the top of the aquifer, see Bjørnarå et al. [4] for details.

### 4. Case study: CO<sub>2</sub> injection at KB-503 in In Salah, Algeria

Here we simulate numerically a simplified version of the CO<sub>2</sub> injection at KB-503 in In Salah, Algeria as our case study to compare the fully resolved solution with the dimensionally reduced model. The case model is inspired by Rutqvist et al. [16], but instead of solving it in three dimensions a plane strain (2D) model is solved where a symmetry plane is defined perpendicular to the horizontal injection line, see Figure 1 (left) for geometry.

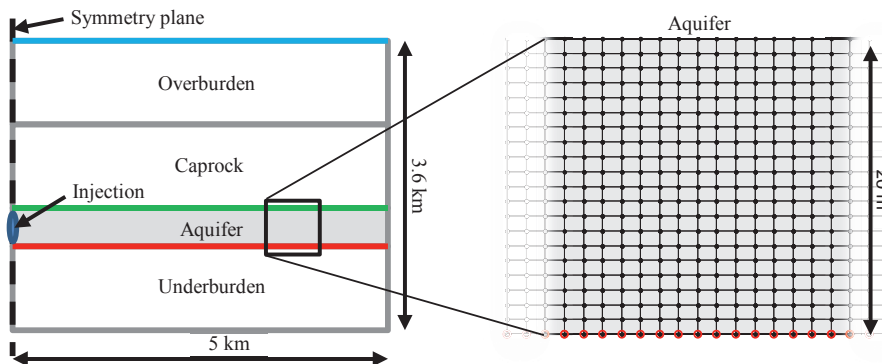


Fig. 1. Left: Geometry sketch of KB-503 injection site in In Salah, Algeria. The colored lines (red, green and blue) indicate the surfaces where the vertical displacement is plotted in Figure 2. Right: Finite element mesh in the aquifer used in the fully resolved model (black dots) and the dimensionally reduced model (red circles).

The model is 3.6 km deep and 5 km wide, which corresponds to 10 km due to the symmetry plane. The CO<sub>2</sub> is injected into a 20 m thick aquifer between a stiff and low permeable mudstone underburden and a carboniferous caprock. The overburden is a low permeable layer consisting of softer cretaceous sandstone and mudstone. The boundaries to the right have a constant pressure value corresponding to initial hydrostatic pressure and no horizontal displacement. The bottom boundary has no-flow conditions and no vertical displacement, and the top boundary has a constant fluid pressure and zero traction. Symmetry boundary conditions are applied to the left boundaries.

The first seven years of injection is simulated with a constant injection rate of 729 ton CO<sub>2</sub>/day. For a 1.5 km long horizontal injection line, this corresponds to 5.62·10<sup>-3</sup> kg/m/s (kg/s CO<sub>2</sub> per meter length of the well). It should be noted that in the fully resolved model the CO<sub>2</sub> is injected along the whole height of the reservoir. In the real application is it injected along a horizontal pipeline, perpendicular to the model plane and should, more appropriately, be modelled as a point source in this plane symmetric model. However, here the length scale of interest is much larger than the near well-bore scale and the aim is to compare the performance of the two approaches. Further, we assume isothermal conditions, no hysteresis in the capillary pressure function and no residual saturation of any of the phases.

Some key material properties are given in Tables 1 and 2. The density of the solid material and Biot's coefficient *b* is 2200 kg/m<sup>3</sup> and 0.7 in all layers, respectively, and the entry pressure *p<sub>d</sub>* for the aquifer is 0.9·10<sup>5</sup> Pa.

Table 1. Mechanical properties used in the case study of KB-503.

Material property	Overburden (0-900m)	Caprock (900-1800m)	Aquifer (1800-1820m)	Underburden (below 1820m)
Youngs modulus, <i>E</i> [GPa]	1.5	20	6	20
Poisson's ratio, <i>ν</i> [-]	0.2	0.15	0.2	0.15
Porosity, <i>φ</i> [-]	0.1	0.01	0.17	0.01
Permeability, <i>k</i> [m <sup>2</sup> ]	1·10 <sup>-17</sup>	1·10 <sup>-19</sup>	13·10 <sup>-15</sup>	1·10 <sup>-19</sup>

Table 2. Fluid and fluid flow properties for brine and CO<sub>2</sub>.

Brine			CO <sub>2</sub>		
Density,	Viscosity,	Compressibility,	Density,	Viscosity,	Compressibility,
$\rho_n$ [kg/m <sup>3</sup> ]	$\mu_n$ [Pa·s]	$c_n$ [1/Pa]	$\rho_n$ [kg/m <sup>3</sup> ]	$\mu_n$ [Pa·s]	$c_n$ [1/Pa]
997	$5.5 \cdot 10^{-4}$	$4.19 \cdot 10^{-10}$	784	$6.9 \cdot 10^{-5}$	$1.56 \cdot 10^{-8}$

Here we apply the dimensional reduction approach to the aquifer, hence it is defined to be semi-confined; water is allowed to leave/enter the aquifer whereas the CO<sub>2</sub> is confined. Thus, the two-phase flow is limited to the aquifer, and in the rest of the model only brine is displacing.

As mention earlier, the motivation to derive an integrated poroelastic two-phase flow formulation is to save degrees of freedom and save computational time. In order to compare the performance between the fully resolved model and dimensionally reduced model a comparable mesh is used, see Figure 1 (right). In this particular case, the fully resolved model has 211 kDOFs while the reduced model has 135 kDOFs, a saving of 36% in computational cost. In computational time, the reduced model solves 2.7 times faster compared to the fully resolved model (or 36% of the solving time of the fully resolved model). Note that a lower resolution is feasible, in both cases, but for the sake of getting a nicely resolved solution, a fairly dense mesh is used.

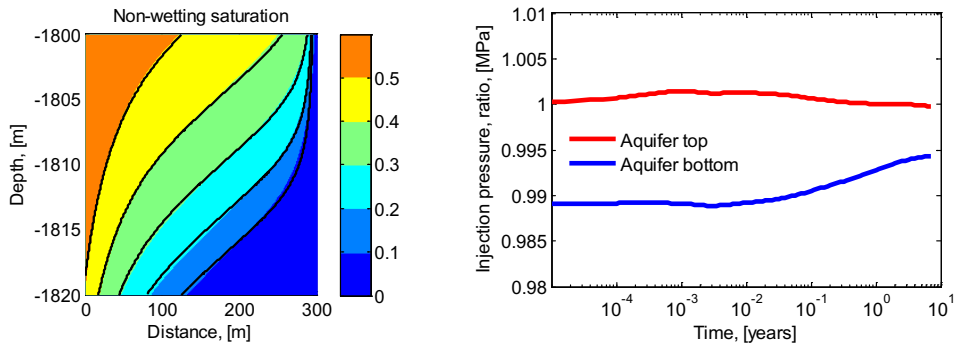


Fig. 2. Left: CO<sub>2</sub> saturation in aquifer after seven years of injection. Solid lines are the corresponding contour lines for the saturation calculated in the dimensionally reduced model. Note that the axis are not to scale. Right: Injection pore pressure ratio; reduced/fully resolved.

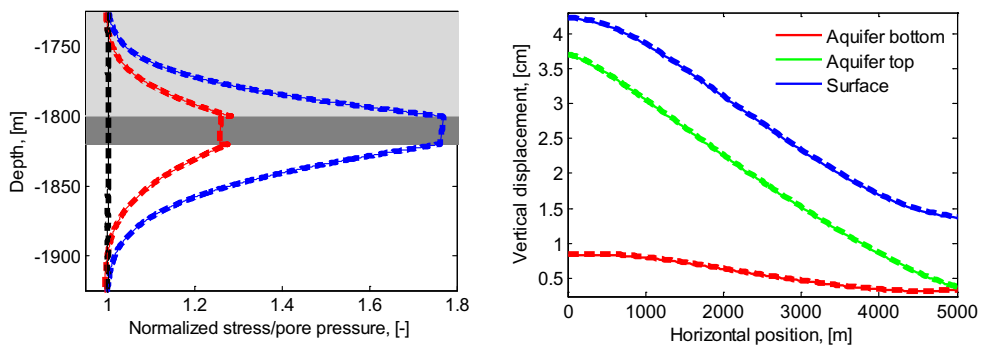


Fig. 3. Left: Vertical profiles of various normalized stress components (normalized to initial values) measured 100 meters away from the symmetry line. Black: vertical stress. Red: horizontal stress. Blue: Pore pressure. Dark gray area indicates the reservoir. Right: Vertical displacement along the bottom of the aquifer (red line), top of aquifer (green line) and surface (surface heave, blue line), cf. Figure 1 (left). In both figure the thin lines are from the simplified model and thick dashed lines are for the fully resolved model.

The saturation profile after seven years of injection for the two approaches are compared in Figure 2 (left) where the colors represent the CO<sub>2</sub> saturation in the fully resolved model and the black lines are the equivalent saturation contour lines for the reduced approach. It can be seen that the reduced model is capable of accurately capturing the CO<sub>2</sub> distribution in the aquifer. In general, the applicability of the reduced approach presented here depends on both the length- and time-scale of interest. For conditions close to the injection point/line, or at short times, the accuracy deteriorates as the underlying assumptions are violated. The match in saturation depends on how fast the phases segregate vertically, and for the dimensionally reduced model; the faster the better. Hence, for very short simulation times, in locations close to the injection point, and if the density difference between the two phases is low or the permeability in the aquifer becomes too low, the VE assumption may no longer be fully justified. However, in the realistic (and challenging) case simulated here, it is well within a very good approximate solution. In Figure 2 (right) the ratio of the pore pressure at the injection point at the top and bottom of the aquifer for the two models are shown, it is close to 1 for the entire simulation time (7 years). The results for the vertical displacement along the faces of the aquifer top and -bottom and the surface in Figure 3 (right) and the Vertical profiles of various normalized stress components (normalized to initial values) in Figure 3 (left) are coinciding for the two approaches.

The limit for the applicability of the reduced approach is case dependent and has not been investigated here. However, it appears (not shown here) that the critical assumption in the dimensionally reduced approach is the VE-assumption, as the poroelastic effect is little affected by mismatch in the saturation profile. The applicability of the VE assumption has been investigated by others, see eg. Court et al. [7].

In this study the simplified model approach through dimensional reduction has proved promising in providing significant savings in computational cost and time (2.7 times faster) when faced with a large number of simulations. It has also been demonstrated that such models can retain reasonable accuracy when applied to realistic field data, such as the conditions at In Salah.

## Acknowledgements

The authors are thankful to the following sponsors for the financial support of this work: Research Council of Norway (through the MatMoRA-II project 215641, Mathematical Modeling and Risk Assessment of CO<sub>2</sub> storage), Statoil ASA, University of Bergen, Durham University and Norwegian Geotechnical institute (NGI).

## References

- [1] Bear J, Corapcioglu MY. Mathematical Model for Regional Land Subsidence Due to Pumping. 2. Integrated Aquifer Subsidence Equations for Vertical and Horizontal Displacements. *Water Resources Research*, 17(4):947–958, August 1981.
- [2] Biot MA. General theory of three-dimensional consolidation. *Journal of Applied Physics*, 12(2):155–164, 1941.
- [3] Bissell RC, Vasco DW, Atbi M, Hamdani M, Okwelegbe M, Goldwater MH. A full field simulation of the In Salah gas production and CO<sub>2</sub> storage project using a coupled geo-mechanical and thermal fluid flow simulator. *Energy Procedia*, 4(0):3290 – 3297, 2011. 10th International Conference on Greenhouse Gas Control Technologies.
- [4] Bjørnarå TI, Nordbotten JM, Mathias SA, Park J, Vertically Integrated Models For Coupled Flow and Deflection in Porous Media, submitted.
- [5] Cavanagh A, Ringrose P. In salah high-resolution heterogeneous simulations of CO<sub>2</sub> storage. *Search and Discovery Article #80092*, July 2010.
- [6] Cavanagh A, Ringrose P. Simulation of CO<sub>2</sub> distribution at the In Salah storage site using high-resolution field-scale models. *Energy Procedia*, 4(0):3730 – 3737, 2011. 10th International Conference on Greenhouse Gas Control Technologies.

- [7] Court B, Bandilla KW, Celia MA, Janzen A, Dobosy M, Nordbotten JM, Applicability of vertical-equilibrium and sharp-interface assumptions in CO<sub>2</sub> sequestration modeling, *International Journal of Greenhouse Gas Control*, 10(0):134-147, 2012
- [8] Durucan S, Shi J-Q, Sinayuc C, Korre A. In salah CO<sub>2</sub> storage JIP: Carbon dioxide plume extension around KB-502 well-new insights into reservoir behaviour at the In Salah storage site. *Energy Procedia*, 4(0):3379 – 3385, 2011. 10th International Conference on Greenhouse Gas Control Technologies.
- [9] Gemmer L, Hansen O, Iding M, Leary S, Ringrose P. Geomechanical response to CO<sub>2</sub> injection at krechba, In Salah, Algeria. *First Break*, 30(2):79–84, February 2012.
- [10] Nordbotten JM, Dahle HK. Impact of capillary forces on large-scale migration of CO<sub>2</sub>. In J. Carrera, editor, 18th Conference on Computational Methods for Water Resources, Barcelona, Spain, 2010.
- [11] Onuma T, Okada K, Otsubo A. Time series analysis of surface deformation related with CO<sub>2</sub> injection by satellite-borne SAR interferometry at In Salah, Algeria. *Energy Procedia*, 4(0):3428 – 3434, 2011. 10th International Conference on Greenhouse Gas Control Technologies.
- [12] Pinder GF, Gray WG. *Essentials of Multiphase Flow and Transport in Porous Media*. John Wiley & Sons, Inc., Hoboken, NJ, USA, 2008.
- [13] Rinaldi AP, Rutqvist J. Modeling of deep fracture zone opening and transient ground surface uplift at KB-502 CO<sub>2</sub> injection well, In Salah, Algeria. *International Journal of Greenhouse Gas Control*, 12(0):155 – 167, 2013.
- [14] Ringrose P, Atbi M, Mason D, Espinassous M, Myhrer Ø, Iding M, Mathieson A, Wright I. Plume development around well KB-502 at the In Salah CO<sub>2</sub> storage site. *First Break*, 27(1):85–89, January 2009.
- [15] Rutqvist J, Liu H-H, Vasco DW, Pan L, Kappler K, Majer E. Coupled non-isothermal, multiphase fluid flow, and geomechanical modeling of ground surface deformations and potential for induced micro-seismicity at the In Salah CO<sub>2</sub> storage operation. *Energy Procedia*, 4:3542–3549, 2011.

- [16] Rutqvist J, Vasco DW, Myer L. Coupled reservoir-geomechanical analysis of CO<sub>2</sub> injection and ground deformations at In Salah, Algeria. *International Journal of Greenhouse Gas Control*, 4(2):225–230, 2010. The Ninth International Conference on Greenhouse Gas Control Technologies.
- [17] Shi J-Q, Sinayuc C, Durucan S, Korre A. Assessment of carbon dioxide plume behaviour within the storage reservoir and the lower caprock around the KB-502 injection well at In Salah. *International Journal of Greenhouse Gas Control*, 7(0):115–126, 2012.
- [18] Zimmerman RW. *Compressibility of Sandstones*. Elsevier, Amsterdam, 1991.